

## Application of the Backward Extrapolation Method for Paralyzable and Non-Paralyzable Dead-Time Corrections in Pulsed Neutron Source Experiments\*

A. Talamo<sup>1</sup> and Y. Gohar

Argonne National Laboratory, 9700 South Cass Avenue, Argonne, IL 60439, USA  
<sup>1</sup>alby@anl.gov

**Abstract** – This work extends the application of backward extrapolation method from stationary to pulsed neutron sources. With the latter external neutron sources, the pulse period is divided into an arbitrary number of time intervals and the neutron counts within a single time interval are corrected using the backward extrapolation method. This correction is applied to all the time intervals of the pulse period.

### I. INTRODUCTION

The dead-time is the minimum time interval  $\delta$  between two successive neutron events (counts) that can be scored by a counting system (e.g. neutron detector). Events occurring during the dead-time are lost and not counted by the neutron detector. Consequently, the experimental signal (neutron counts) of a neutron detector needs a correction to account for the dead-time effect. Neutron detectors operating in pulse mode are subjected to the dead-time effect, while neutron detectors operating in current mode are not subjected to the dead-time effect [1].

Generally, the non-paralyzable and paralyzable models of dead-time are used to correct the experimental signal of a neutron detector for the dead-time effect [2]. In the paralyzable model, the dead-time starts at each neutron count. In the non-paralyzable model, the dead-time first starts at one neutron count and then at the next neutron count that occurs after a time interval larger than the dead-time (Fig. 1). Consequently, the corrected (real) neutron counts value obtained by the paralyzable model has a higher value relative to that from the non-paralyzable model (Fig. 2).

Dubi et al. [2] have applied the backward extrapolation method to estimate the dead-time value when the average value of the neutron counts does not vary with time. In this case, the subcritical assembly is driven by a stationary external neutron source (e.g. californium). In the backward extrapolation method, a set of fictitious dead-time values (e.g. from 0 to 100  $\mu$ s with 0.1  $\mu$ s bin) is assumed for the detector. For each fictitious value of the dead-time, the detector experimental signal (e.g. neutron captures timestamps) is corrected by applying the paralyzable or the non-paralyzable correction, as illustrated in Fig. 1.

This work adapts the backward extrapolation method to pulsed neutron source experiments. In these experiments, a particle accelerator operating in pulsed

mode ejects particles for a short time interval (pulse duration) and repeats this ejection at a fixed time interval (pulse period  $T$ ). Typical values of the pulse duration and period range from 5 to 10 microseconds ( $\mu$ s) and from 20 to 50 milliseconds (ms), respectively. The pulse period must be long enough to allow prompt neutrons to decay and short enough to have a constant contribution from delayed neutrons.

### II. DEAD-TIME CORRECTION FOR STATIONARY EXTERNAL NEUTRON SOURCES

Equations 1 and 2 relate the measured count rate  $m$  (in counts per second) to the real counts rate  $c$  (in counts per second) for the non-paralyzable and paralyzable model, respectively [1]. In these equations, it is assumed that the dead-time is known and that the average neutron counts per second is constant over time.

$$c \cong \frac{m}{1 - m\delta} \quad (1)$$

$$m \cong c \cdot \exp(-c\delta) \quad (2)$$

Typically, the dead-time is measured by performing four experiments using two californium neutron sources with strengths  $A$  and  $B$  [3]. In the first experiment, the neutron counts ( $m_{sf}$ ) come from the background neutron source, due to the spontaneous fission events in the fuel material. In the second and third experiments, the neutron counts ( $m_A$  and  $m_B$ ) come from the  $A$  and  $B$  external neutron sources, separately. In the fourth experiment, the neutron counts ( $m_{AB}$ ) come from both the  $A$  and  $B$  external neutron sources, simultaneously. Equations 3 to 6 apply to the four experiments, respectively.

$$c_{sf} \cong \frac{m_{sf}}{1 - m_{sf}\delta} \cong m_{sf} \quad (3)$$

$$c_A + c_{sf} \cong \frac{m_A}{1 - m_A\delta} \cong m_A(1 + m_A\delta) \quad (4)$$

\*The submitted manuscript has been created by UChicago Argonne LLC, Operator of Argonne National Laboratory ("Argonne"). Argonne, a U.S. Department of Energy Office of Science laboratory, is operated under Contract No. DE-AC02-06CH11357. The U.S. Government retains for itself, and others acting on its behalf, a paid-up nonexclusive, irrevocable worldwide license in said article to reproduce, prepare derivative works, distribute copies to the public, and perform publicly and display publicly, by or on behalf of the Government.

$$c_B + c_{sf} \cong \frac{m_B}{1 - m_B \delta} \cong m_B (1 + m_B \delta) \quad (5)$$

$$c_A + c_B + c_{sf} \cong \frac{m_{AB}}{1 - m_{AB} \delta} \cong m_A (1 + m_{AB} \delta) \quad (6)$$

In Eqs. 3 to 6 the subscript denotes the strength of the external neutron source. In Eq. 3, it is assumed that the counting rate from the spontaneous fission neutron source

(from the fuel material) is small enough to neglect dead-time effects. In Eqs. 4 to 6, it is assumed that the dead-time value is small enough to simplify the term  $1/(1-m\delta)$  as  $1+m\delta$ . The dead-time value can be obtained by Eq. 7, which solves the equations system formed by Eqs. 3 to 6.

$$\delta \cong \frac{m_A + m_B - m_{AB} - m_{sf}}{m_{AB}^2 - m_A^2 - m_B^2} \quad (7)$$

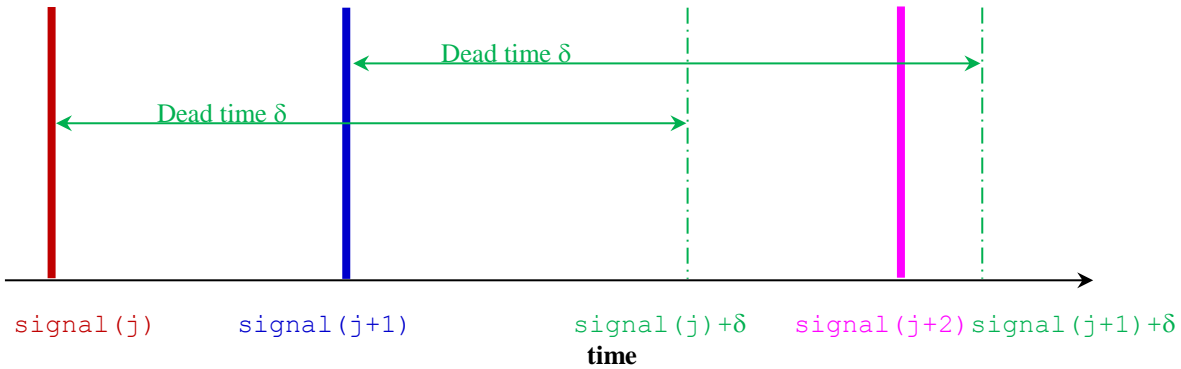


Fig. 1. Illustration of the dead-time effect; signal in the time scale indicates a neutron detector count (ionization); in the non-paralyzable model, the detector scores signal(j) and signal(j+2) because signal(j+2) is greater than signal(j)+delta; in the paralyzable model, the detector only scores signal(j) because signal(j+2) is smaller than signal(j+1)+delta; in both models the detector does not score signal(j+1) because it is smaller than signal(j)+delta.

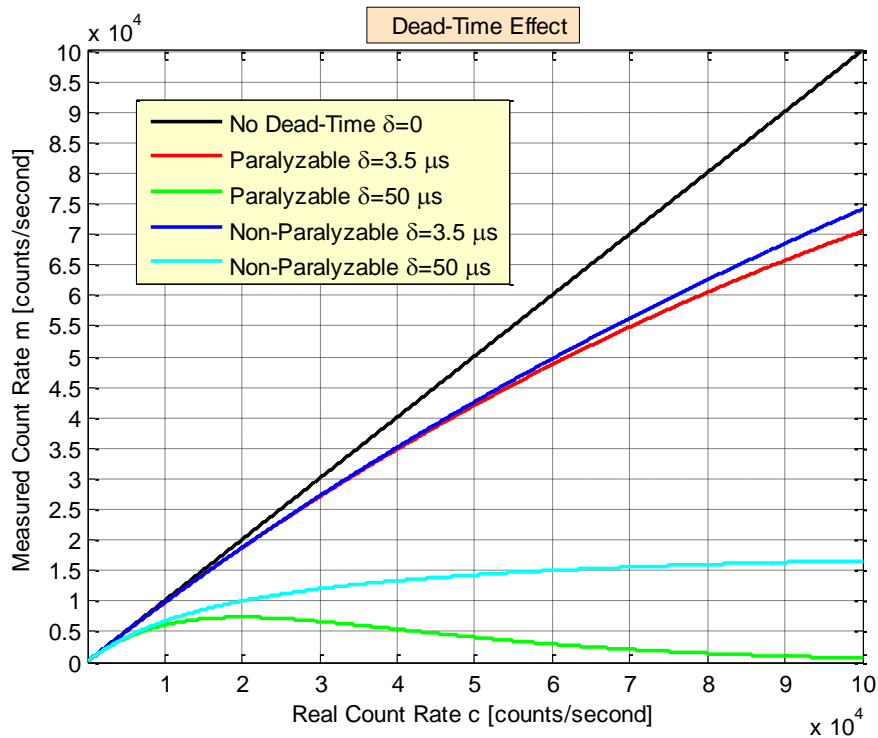


Fig. 2. Illustration of the dead-time effect for delta equal to 3.5 and 50 microseconds when the average intensity of the neutron source is constant over time (the curves use Eqs. 1 and 2).

An alternative method to determine the dead-time is the backward extrapolation method discussed in Section I.

### III. THE YALINA THERMAL FACILITY

All experiments presented in this work have been performed with the YALINA thermal facility. This nuclear assembly has polyethylene moderator and EK10 fuel rods with 10% enriched uranium [4]. The fuel unit cell, the target, and fuel zones have a square geometry with side 2, 8 and 40 cm, respectively. The axial reflectors consist of borated polyethylene blocks. In the present study, the configuration of the facility has been modified, relative to the one used in previous studies [5], by removing the experimental channels in the fuel region and by inserting a borated polyethylene axial reflector on the beam tube side. In the YALINA thermal configurations studied in this work, the fuel zone has symmetric axial reflectors.

On one side of the fuel rods, the deuteron beam tube penetrates the assembly and is surrounded by air. The radial reflector consists of a 40 cm thick graphite block. An organic glass layer covers the vertical outer surfaces of the graphite reflector. The other two external sides (top and bottom) of the radial graphite reflector are covered with thin layers made of cadmium and iron; the iron layer lies on the outside. In addition, a thin (0.4 cm thick) organic glass layer covers the end of the fuel zone on the beam tube side. The active and total fuel lengths are 50 and 59 cm, respectively. The facility is equipped with three emergency shut down control rods, which are always withdrawn during the experiments.

In the experiments presented in this study, the YALINA Thermal subcritical assembly has been driven either by a californium neutron source or by a deuterium-deuterium (D-D) pulsed neutron source with 5  $\mu$ s duration and 14.2 ms period. The particle accelerator emits deuterons with 250 keV energy. Figure 3 illustrates the facility. The number of loaded fuel rods is 288 and 188 for the californium and D-D external neutron source, respectively.

### IV. MCNP MODEL

The YALINA Thermal facility has been modeled in detail using the Monte Carlo MCNP code [6], as illustrated in Figs. 4 to 6. MCNP records the timestamp, when a detector neutron capture occurred, in the PTRAC output file. However, in the original version of MCNP, the neutron capture timestamp does not take into account the time when the neutron was emitted by the external neutron source. This issue was solved by applying the following patch to the `ptrak.F90` file (line 168) of MCNP version 6.1.1 beta version.

```
168c168
<
write(iupw,'(i10,lpe15.5,7i8)')nps,pbl%r%tm
e-pbl_src%r%tme,ic,kn(1), &
---
>
write(iupw,'(i10,lpe35.25,7i8)')nps,pbl%r%t
me,ic,kn(1), &
```

The above patch also increases the precision of the neutron capture timestamp, since the original version of MCNP has low precision (up to the millisecond). Appendix A of this paper gives an example of the MCNP input deck to obtain the timestamps of the  $^3\text{He}$  neutron captures in cell 1700 defining the gas region of the neutron detector for a subcritical assembly driven by a D-D neutron source. In order to obtain the neutron capture timestamps, the `ptrac` card must be coupled to the `F8` tally card. The `ptrac` card requires analog captures, no variance reduction techniques and serial computations (no MPI or OPENMP parallel computing platforms). However, the results of multiple serial computations can be easily combined together if each computation starts with a different random number seed using the `rand` card. Processing the PTRAC data with MATLAB scripts requires the MCNP output data to be sorted in increasing order. This task can be easily accomplished by using the `sort` MATLAB function.

The possibility to obtain the detector timestamps is a unique feature of Monte Carlo neutron transport codes. With deterministic codes, it is not possible to obtain this data.

## V. RESULTS

### 1. Californium Neutron Source

Figures 7 and 8 gives an example of the backward extrapolation method applied to the detector signals from MC1 and EC6 experimental channels. In these experiments, the YALINA Thermal facility was driven by a californium neutron source. The real dead-time value of the neutron detector can be identified by the right edge of the lavender area. The latter marks the region where the neutron counts value does not depend on the fictitious dead-time. All the experimental channels of the facility are illustrated in Figs. 4 to 6. In Figs. 7 and 8, the fictitious dead-time ranges from 0.1 to 100  $\mu$ s with 0.1  $\mu$ s interval.

According to the results obtained by the application of the backward extrapolation method, the helium and fission chambers detectors used in the YALINA Thermal experiments have 3.5 and 0.5  $\mu$ s dead-time, respectively.



Fig. 3. Illustration of the YALINA Thermal facility. Source: Argonne National Laboratory staff.

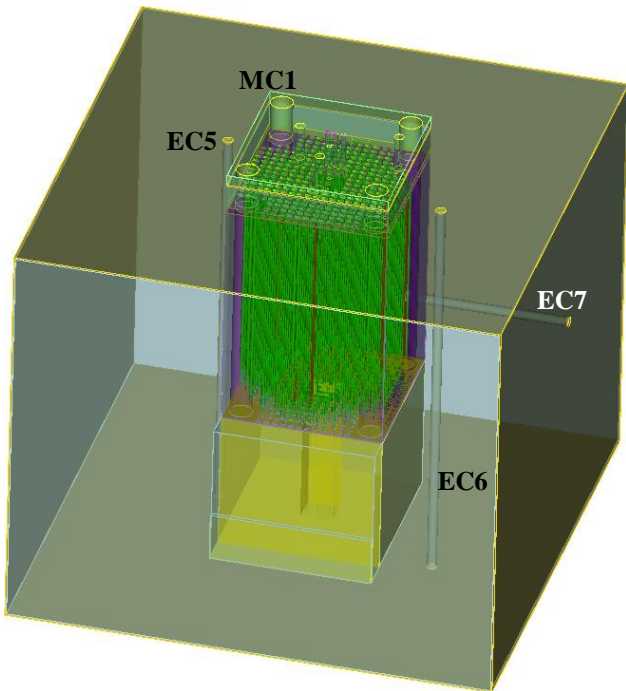


Fig. 4. Overview of the MCNP model of the YALINA Thermal facility.

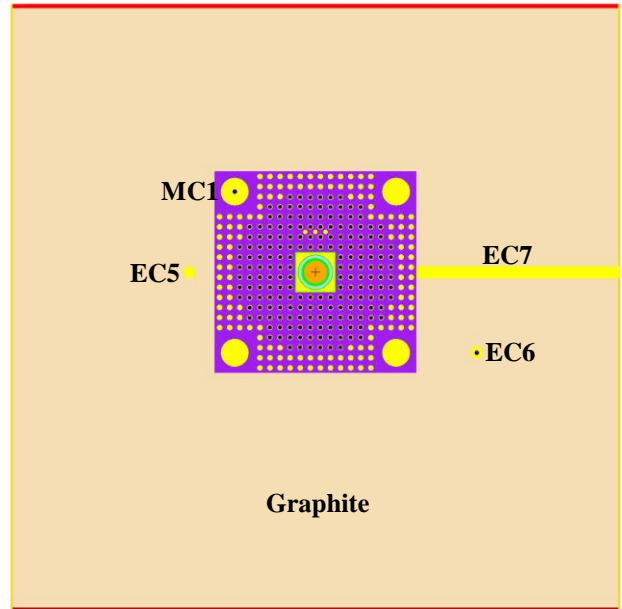


Fig. 5. Vertical section of the MCNP model of the YALINA Thermal facility loaded with 188 fuel rods.

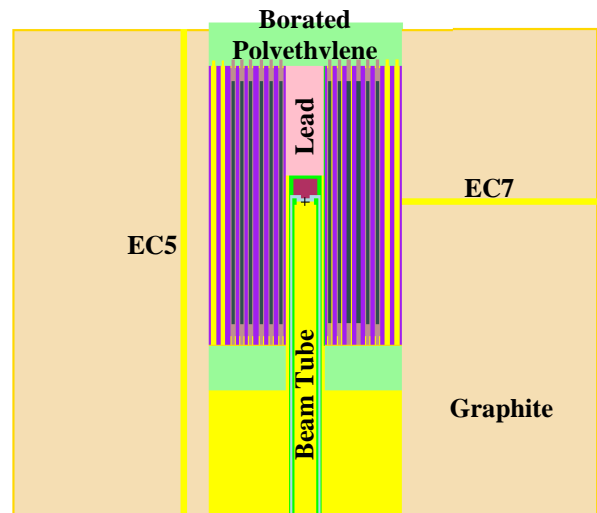


Fig. 6. Horizontal section of the MCNP model of the YALINA Thermal facility loaded with 188 fuel rods.

The real counts per second can be obtained by fitting the measured counts per second, as a function of the fictitious dead-time, in the range where the latter exhibit a slope. The data from the EC6 experimental channel can be fitted by a linear function, as shown in Fig. 9. The value assumed by the fitting function for the fictitious dead-time equal to zero represents the real counts per second (894.78 counts/s). The latter value is slightly higher than the measured counts per second (891.73 counts/s).

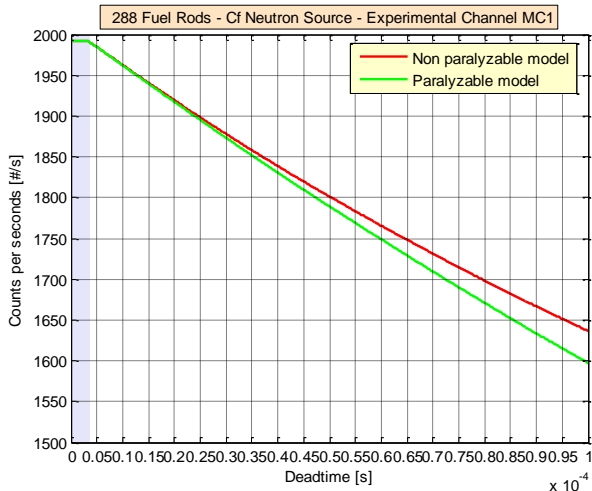


Fig. 7. <sup>3</sup>He neutron captures per second, in the experimental channel MC1 as a function of fictitious dead-time.

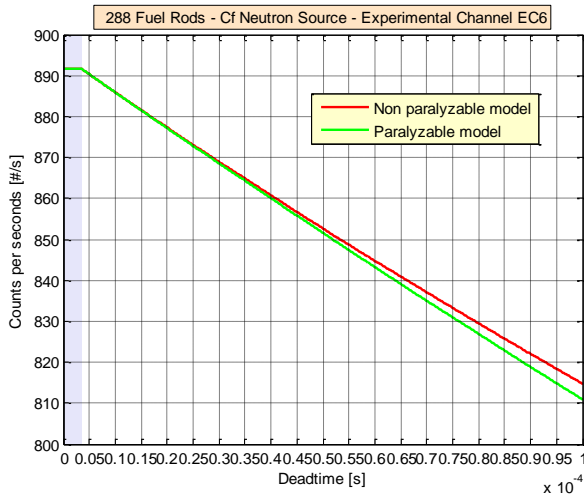


Fig. 8. <sup>3</sup>He neutron captures per second, in the experimental channel EC6 as a function of fictitious dead-time.

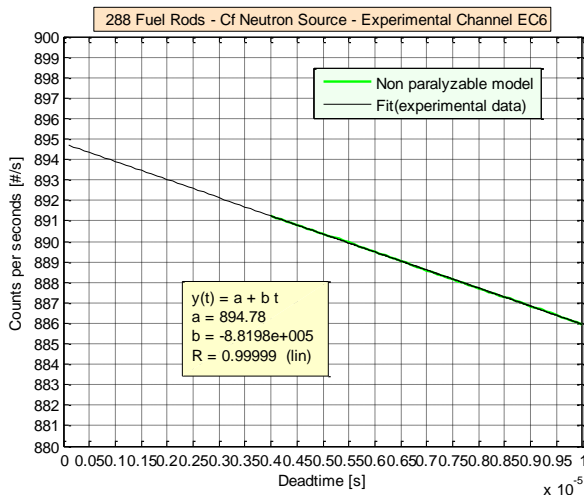


Fig. 9. Fitting of the <sup>3</sup>He neutron captures per second in the experimental channel EC6.

## 2. Pulsed Neutron Source

This work extends the application of the backward extrapolation method to pulsed neutron source experiments. The YALINA Thermal subcritical assembly is driven by a particle accelerator, operating in pulsed mode, rather than by a californium neutron source. In this case, Eqs. 1 and 2 cannot be applied because the neutron count rate is not constant. Typically, the particle accelerator delivers a neutron pulse for 5 to 10  $\mu$ s (pulse duration) and repeats the pulse every 20 to 50 ms (pulse period). For pulsed neutron sources, the backward extrapolation method can be implemented by applying the following procedure.

- 1) The pulse period (e.g. 14 ms) is divided into many intervals (e.g. 140 intervals with 0.1 ms width).
- 2) A set of fictitious dead-time values (e.g. from 0 to 100  $\mu$ s with 0.1  $\mu$ s bin) is imposed to the detector measured neutron counts ( $m$ ) in each interval.
- 3) The detector measured neutron counts ( $m$ ) within an interval is plotted as a function of the fictitious dead-time (e.g. Fig. 10).
- 4) The neutron count ( $c$ ) is obtained by extrapolating the curve fitting the detector measured neutron counts ( $m$ ) for a fictitious dead-time value equal to zero (e.g. Fig. 11).
- 5) The procedures of the third and fourth steps are repeated for all neutron counts values of each interval of the first step and the real neutron count ( $c$ ) is obtained as a function of time.

Fig. 10 illustrates this procedure for the first pulse interval, which ranges from 0 to 0.1 ms. The data shown in Fig. 10 can be fit by an exponential function, as illustrated in Fig. 11, and the real neutron counts ( $c$ ) is obtained as the value of the fit function (black curve) when the fictitious dead-time is equal to zero.

Figures 12 to 15 illustrate the application of the backward extrapolation method for the second and third time intervals, which range from 0.1 to 0.2 ms and from 0.2 to 0.3 ms, respectively. Similar procedures were repeated for the remaining 137 intervals (the total number of intervals is 140). By using 140 different fitting functions, it is possible to calculate the corrected (real) neutron counts per second value for all the 140 intervals. This is accomplished by calculating the value of the fitting function at the fictitious dead-time equal to zero.

As expected from Fig. 2, the measured counts per second using the paralyzable model of dead-time is lower relative to the value obtained using the non-paralyzable model (Figs. 10, 12, and 14). When  $\delta$  is a few  $\mu$ s and up to 10,000 counts per second, the real and measured counts per second values are very close, independently of the dead-time model (paralyzable or non-paralyzable), as shown in Fig. 2.

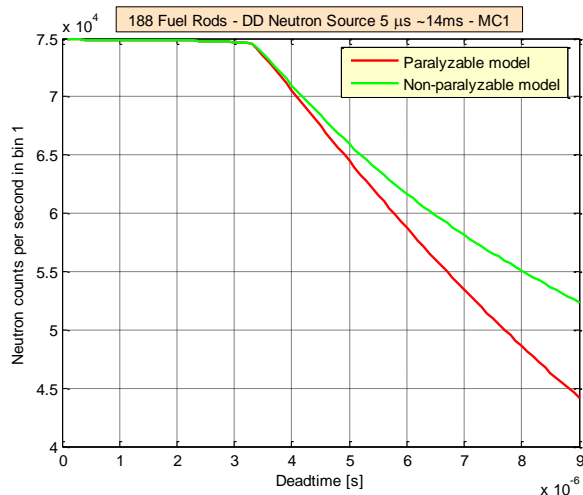


Fig. 10. Neutron counts in the first time interval (between 0 and 0.1 ms) as a function of the fictitious dead-time.

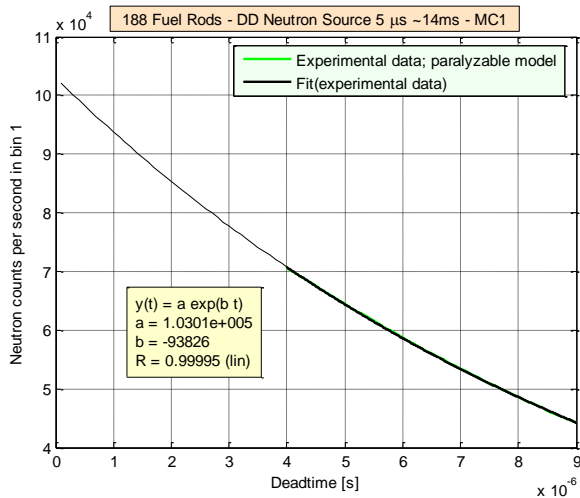


Fig. 11. Fitting of the neutron counts in the first time interval (between 0 and 0.1 ms) for the paralyzable model.

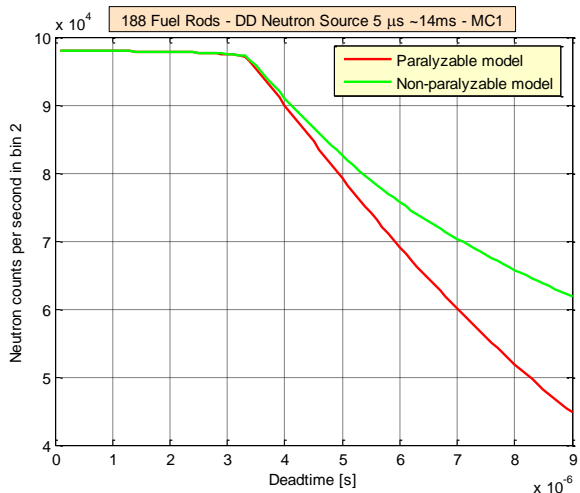


Fig. 12. Neutron counts in the second time interval (between 0.1 and 0.2 ms) as a function of the fictitious dead-time.

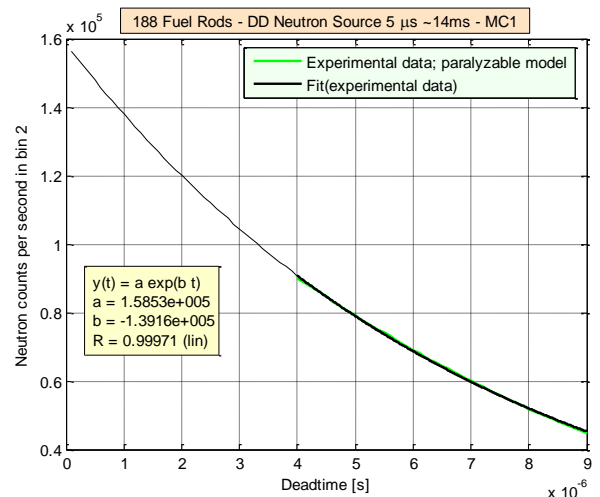


Fig. 13. Fitting of the neutron counts in the second time interval (between 0.1 and 0.2 ms) for the paralyzable model.

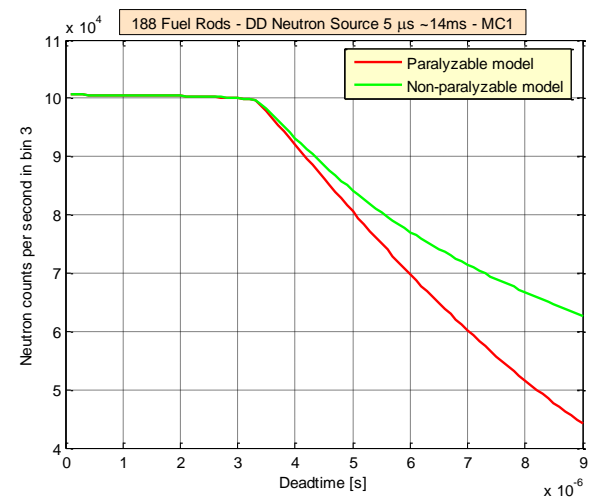


Fig. 14. Neutron counts in the third time interval (between 0.2 and 0.3 ms) as a function of the fictitious dead-time.

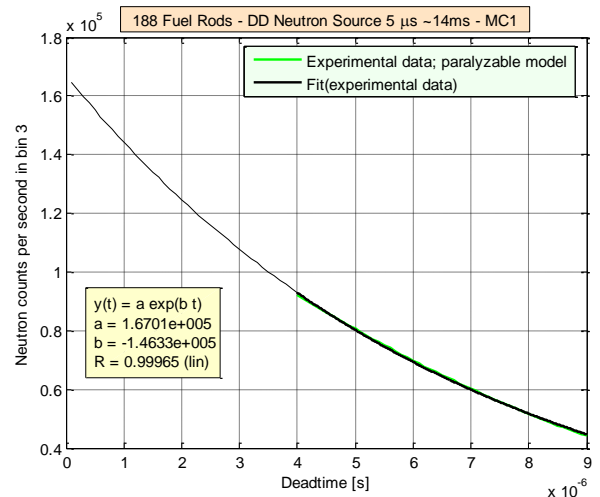


Fig. 15. Fitting of the neutron counts in the third time interval (between 0.2 and 0.3 ms) for the paralyzable model.

Figure 16 plots the neutron counts ( $c$ ) as a function of time during the pulse period. Both the paralyzable and the non-paralyzable dead-time models have been used in the backward extrapolation method. As previously discussed, the corrected (real) neutron counts are higher for the paralyzable model relative to the non-paralyzable model.

In addition, the neutron counts values have also been obtained by a MCNP computer simulation that takes into account the equilibrium condition of delayed neutrons [1,7-9]. Figure 16 shows that the application of the backward extrapolation method to the experimental data improves the comparison between experimental and computational data.

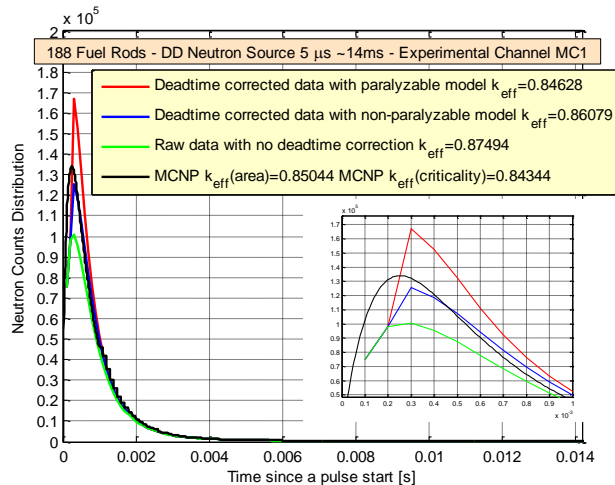


Fig. 16.  $^3\text{He}$  neutron captures per second as a function of time in the experimental channel MC1 of the YALINA Thermal facility driven by a Deuterium-Deuterium pulsed neutron source during the pulse period (14.2 ms).

The effective multiplication factor  $k_{eff}$  can be obtained by applying the area method [1] to all the four curves plotted in Fig. 16. The effective multiplication factor obtained by experimental and computational data is reported in the legend of Fig. 16. For this set of YALINA Thermal experiments the dead-time impact on the  $k_{eff}$  value is within few thousands pcm.

In addition to the dead-time correction, the effective multiplication factor must be also corrected to take into account the detector position and type [10,11].

## VI. CONCLUSIONS

The backward extrapolation method can be applied not only to stationary but also to pulsed neutron sources experiments. In the latter case, the pulse period is divided into an arbitrary number of time bins and a fictitious dead-time value is imposed to the counts per second in each time bin. Then, the real counts per second is obtained as the value of the fitting function at ( $m_{AB}$ ) the fictitious dead-time equal to zero.

## APPENDIX A: MCNP INPUT

```

mode n
print 40 50 60 72 98 102 115 120
lost 1
nps 10e6
c tally runtpe mctal runtpe rendezvous
prmdp 2e6 2e6 0 1 2e6
phys:n 30 30 $ upper energy cutoff 30 MeV - analog capture
cut:n 500e8 0 0 0
ptrac buffer=1000 file=asc max=2e9 write=all coinc=lin
event=cap type=n tally=8
rand seed=17373738176025
sdef pos=0 0 0
    axs=0 0 1
    vec=0 0 1
    rad=d1
    ext=d2
    dir=d3
    erg=fdir d4
    tme=d5
si1 h 0 0.235
sp1 -21 1
si2 h 0 0.1
sp2 -21 0
c Deuterium-Deuterium Neutron Source
c Handbook on Nuclear Activation Data, Technical Reports Series
c No.273, p. 116, IAEA, Vienna (1987).
c energy-angle distribution for d+d reaction 250 keV
si3 a -1. -.966 -.866 -.707 -.500 -.259 0
    .259 .5 .707 .866 .966 1
sp3 4.75 4.5 4.1 3.6 3.0 2.5 2.3
    2.5 3.2 4.25 5.7 6.9 7.3
ds4 2.01 2.03 2.07 2.14 2.24 2.37 2.51
    2.66 2.80 2.94 3.04 3.11 3.14
si5 h 0 500 500e8
sp5 d 0 1 0
c TALLY CARDS
f8:n 1700
fc8 PTRAC TALLY
ft8 cap -1 -1 2003
    
```

## ACKNOWLEDGMENTS

This work is supported by the U.S. Department of Energy, Office of Material Management and Minimization (M3), National Nuclear Security Administration.

## REFERENCES

1. A. TALAMO and Y. GOHAR, "Neutron Detector Signal Processing to Calculate the Effective Neutron Multiplication Factor of Subcritical Assemblies," Argonne National Laboratory, [ANL-16/14](#), (2016).
2. C. DUBI et al. "Evaluating Dead Time Corrections in Reactor Neutrons Detector Readings Using the Backward Extrapolation Method," PHYSOR, Sun Valley, ID, USA, (2016).
3. A.E. PROFIO, "Experimental Reactor Physics," John Wiley and Sons, ISBN-13: 978-0471700951, pp. 160-167, 1976.

4. A. TALAMO et al., "Correction Factor for the Experimental Prompt Neutron Decay Constant," [Annals of Nuclear Energy](#) **62**, pp. 421-428, (2013).
5. A. TALAMO et al., "Monte Carlo and Deterministic Neutronics Analyses of YALINA Thermal Facility and Comparison with Experimental Results," Nuclear Technology **184/2**, pp. 131-147, 2013.
6. D.B. PELOWITZ et al., "MCNP6 User's Manual, Code Version 6.1.1beta," Los Alamos National Laboratory, LA-CP-14-00745, (2014).
7. A. TALAMO et al., "Pulse Superimposition Computational Methodology for Estimating the Subcriticality Level of Nuclear Fuel Assemblies," [Nuclear Instruments and Methods in Physics Research A](#) **606/3**, pp. 661-668, 2009.
8. A. TALAMO, Y. Gohar and C. Rabiti, "Monte Carlo Modeling and Analyses of YALINA-Booster Subcritical Assembly Part II: Pulsed Neutron Source," Argonne National Laboratory, [ANL-08/33](#), 2008.
9. A. TALAMO and Y. GOHAR, "Numerical Application of the Sjöstrand Method without the Pulses Superimposition Methodology," [ANS Winter Meeting](#), Washington, DC, USA, 2015.
10. A. TALAMO et al., "Monte Carlo and Deterministic Calculation of the Bell and Glasstone Spatial Correction Factor," [Computer Physics Communications](#) **183/9**, pp. 1904-1910, 2012.
11. A. TALAMO et al., "Impact of the Neutron Detector Choice on Bell and Glasstone Spatial Correction Factor for Subcriticality Measurement," [Nuclear Instruments and Methods in Physics Research A](#) **668**, pp. 71-82, 2012.